Distinguishing pancreatic cancer and autoimmune pancreatitis with in vivo tomoelastography

Liang Zhu[1] · Jing Guo[2] · Zhengyu Jin[1] · Huadan Xue[1] · Menghua Dai[3] · Wen Zhang[4] · Zhaoyong Sun[1] · Jia Xu[1] · Stephan R. Marticorena Garcia[2] · Patrick Asbach[2] · Bernd Hamm[2] · Ingolf Sack[2]

Abstract

Objectives To prospectively investigate the stiffness and fluidity of pancreatic ductal adenocarcinoma (PDAC) and autoimmune pancreatitis (AIP) with tomoelastography, and to evaluate its diagnostic performance in distinguishing the two entities.

Methods Tomoelastography provided high-resolution maps of shear wave speed (c in m/s) and phase angle (φ in rad), allowing mechanical characterization of the stiffness and fluidity properties of the pancreas. Forty patients with untreated PDAC and 33 patients with untreated AIP who underwent diagnostic pancreatic MRI at 3-T together with multifrequency MR elastography and tomoelastography data processing were prospectively enrolled. Ten healthy volunteers served as controls. Two radiologists and a technician measured pancreatic stiffness and fluidity independently. The two radiologists also independently evaluated the patients' conventional MR sequences using the following diagnostic score: 1, definitely PDAC; 2, probably PDAC; 3, indeterminate; 4, probably AIP; and 5, definitely AIP. Interobserver agreement was assessed. Stiffness and fluidity of PDAC, AIP, and healthy pancreas, as well as diagnostic performance of tomoelastography and conventional MRI, were compared.

Results AIP showed significantly lower stiffness and fluidity than PDAC and significantly higher stiffness and fluidity than healthy pancreas. Pancreatic fluidity was not influenced by secondary obstructive changes. The intraclass correlation coefficient for pancreatic stiffness and fluidity by the 3 readers was near-perfect (0.951–0.979, all $p < 0.001$). Both stiffness and fluidity allowed distinguishing PDAC from AIP. AUCs were 0.906 for stiffness, 0.872 for fluidity, and 0.842 for conventional MRI.

Conclusions Pancreatic stiffness and fluidity both allow differentiation of PDAC and AIP with high accuracy.

Key Points

• *AIP showed significantly lower stiffness and fluidity than PDAC and significantly higher stiffness and fluidity than healthy pancreas.*
• *Both stiffness and fluidity allowed distinguishing PDAC from AIP.*
• *Pancreatic fluidity could distinguish malignancy from non-malignant secondary obstructive changes.*

Keywords Pancreatic ductal adenocarcinoma · Autoimmune pancreatitis · MRI · Elastography

---

Liang Zhu and Jing Guo contributed equally to this work.

✉ Zhengyu Jin
  jin_zhengyu@163.com

[1] Department of Radiology, Peking Union Medical College Hospital, Beijing, China

[2] Department of Radiology, Charité – Universitätsmedizin Berlin, corporate member of Freie Universität Berlin, Humboldt-Universität zu Berlin, and Berlin Institute of Health, Berlin, Germany

[3] Department of General Surgery, Peking Union Medical College Hospital, Beijing, China

[4] Department of Rheumatology, Peking Union Medical College Hospital, Beijing, China

Abbreviations

AIP	Autoimmune pancreatitis
AUC	Area under the curve
CI	Confidence interval
ICC	Intraclass correlation coefficient
MRE	Magnetic resonance elastography
PDAC	Pancreatic ductal adenocarcinoma
ROC	Receiver operating characteristics

Introduction

Pancreatic ductal adenocarcinoma (PDAC) is a highly lethal malignancy, with the highest 5-year mortality of all solid malignant tumors [1]. Autoimmune pancreatitis (AIP) is an autoimmune-mediated inflammatory disease that attacks the pancreas. It often causes tumor-like swelling of the pancreas and obstructive symptoms, resulting in a clinical profile and radiological appearance highly resembling pancreatic cancer [2]. Since the treatment strategies and prognosis are absolutely different, it is of great importance to distinguish these two disease entities. However, the differential diagnosis remains challenging nowadays [3, 4]. Although serum CA19-9 is elevated in the majority of patients with pancreatic cancer, for the Lewis antigen-negative individuals, which composed approximately 5–10% of the population, serum CA19-9 often remains normal even at the presence of pancreatic cancer [5]. The pooled sensitivity and specificity of CA19-9 for diagnosing pancreatic cancer are 79–81% and 82–90%, respectively [6]. Serum IgG4 is usually normal in type 2 AIP and could be elevated in patients with pancreatic cancer [7–9]. Some radiological signs at contrast-enhanced CT and MRI have been considered useful in differentiating AIP from PDAC; however, the reported interobserver agreement and diagnostic accuracy was variable [10–16]. The diagnostic accuracy with radiological signs could be quite low with inexperienced observers [17].

The mechanical properties of the pancreas provide new insight for disease characterization. Pancreatic cancer is characterized by dense fibrosis induced by fibroblast activation and collagen deposition within the tumor [18]. AIP is characterized by periductal lymphoplasmacytic infiltration and storiform fibrosis [19]. Both the increased cell density and fibrosis alter the tissue's mechanical properties. A preliminary study has shown significant differences in pancreatic stiffness between pancreatic cancer and AIP, which could be used for the differentiation of the two entities [20]. Tomoelastography, a multifrequency magnetic resonance elastography (MRE) technique with noise-robust data postprocessing, has been introduced to the field of cancer imaging recently [21, 22]. It provides high-resolution parametric maps, quantifying tissue stiffness and fluidity. While stiffness is well known as the property assessed by palpation, fluidity is relatively new to tumor characterization, which signifies the conversion of solid behavior into fluid behavior of the tissue, over a continuous range of values from 0 to $\pi/2$. Materials with $\varphi < \pi/4$ have predominantly solid behavior and materials with $\varphi > \pi/4$ have predominantly fluid behavior. The use of tomoelastography and the role of fluidity in characterizing pancreatic lesions have not been explored so far. Therefore, in this prospective study, we investigated the stiffness and fluidity of PDAC and AIP using tomoelastography and determined its diagnostic performance in differentiating PDAC from AIP.

Materials and methods

Study population

This prospective study was approved by the Institutional Review Board, and all patients provided written informed consent. From September 2018 to December 2019, patients with pancreatic lesions suspected to be AIP or pancreatic cancer were prospectively enrolled. Inclusion criteria were as follows: (1) diagnosis of AIP based on the International Consensus Diagnostic Criteria (ICDC), or diagnosis of PDAC based on histopathological findings; (2) patient did not receive any treatment before the MR examination; (3) a full diagnostic pancreatic MRI was performed together with tomoelastography. Patients were excluded for the following reasons: a final diagnosis other than AIP or PDAC ($n = 9$); suspected PDAC without pathological proof ($n = 4$); neoadjuvant chemotherapy for pathologically proven PDAC before the MR examination ($n = 2$); or short-term steroid trial before the MR examination ($n = 3$).

A group of 10 healthy volunteers examined by the same MR protocol but without contrast medium administration were included as controls. They had no history of excessive alcohol consumption, acute pancreatitis, or chronic pancreatitis. Their family history of pancreatic disease was also negative. None of the subjects had any symptoms which might be related to pancreatic diseases, and their MR examinations did not reveal any pancreatic lesion.

Imaging technique

MR sequences

The MR examinations were performed on a 3-T MR imaging system (MAGNETOM Skyra, Siemens Healthcare), using an 18-channel phased-array surface coil. The protocol was identical for all patients, which included axial volume-interpolated breath-hold (VIBE) T1WI, axial turbo spin-echo (TSE) fat-saturated (fs) T2WI, axial and coronal half-Fourier acquisition single-shot turbo spin-echo (HASTE) T2WI, fat-suppressed diffusion-weighted imaging (DWI) with single-shot echo-

planar imaging (EPI), magnetic resonance cholangiopancreatography (MRCP, 3D isotropic acquisition, and 2D single-shot thick-slab acquisition), and the dynamic contrast-enhanced (DCE) time-resolved imaging with interleaved stochastic trajectories (TWIST)-VIBE. Details of sequence parameters are listed in Table 1.

In vivo pancreatic tomoelastography was performed before intravenous contrast agent administration. Multifrequency harmonic vibrations were generated by four compressed air-driven pressure pads, each $8.0 \times 4.0 \times 1.0$ cm^3 in size, placed at the level of the surface projection of the pancreas (2 pads on the anterior side and 2 on the posterior side). Multifrequency wavefield data was acquired using a single-shot, spin-echo EPI sequence with flow-compensated motion-encoding gradients (MEG) during free-breathing. Three-dimensional wave fields were sampled at eight equally spaced time instances for four mechanical frequencies from 30 to 60 Hz with 10-Hz increment sequentially. The MEG frequencies were 37.26 Hz, 37.26 Hz, 37.48 Hz, and 44.88 Hz for the vibration frequencies of 30 Hz, 40 Hz, 50 Hz, and 60 Hz, respectively; the MEG amplitude was 35 mT/m.

Tomoelastography data postprocessing

Multifrequency wave field data was processed using the processing pipeline available at https://bioqic-apps.charite.de. Full field-of-view high-spatial resolution maps of shear wave speed (c) and loss angle of the complex shear modulus (φ) were generated using a multifrequency wave number–based processing algorithm (k-MDEV) [23] and Laplacian operators-based processing method (MDEV) [24]. As described in recent studies using tomoelastography [25, 26], shear wave speed is referred to as a surrogate marker of stiffness as it is directly linked to the magnitude of the complex

shear modulus. Fluidity parameter φ relates to pure fluid properties of the tissue. φ ranges from 0 to $\pi/2$, marking a fluidity transition for solid to fluid [22].

Image analysis

Two radiologists (L.Z. and J. X., with 10 and 6 years of experience in abdominal MRI, respectively) and a technician (Z.S., with 10 years of experience in clinical MR scanning) participated in image evaluation, using the ImageJ software (Version 1.51). The image datasets of the patients and healthy volunteers were anonymized and assigned with a case number in random order. The gender, age, and clinical information were all blinded to the readers. Each reader makes the following evaluations independently.

First, based on stiffness characteristics, the pancreatic involvement pattern was determined as type 1, single-focal "hotspot" lesion on the c map; type 2, multi-focal (≥ 2) "hotspot" lesions; type 3, heterogenous pancreas texture without identifiable focal lesions; and type 4, homogenous pancreas texture without identifiable focal lesions on the c map.

Second, free-hand ROIs were drawn directly on the c maps and then directly transferred to the φ maps. The entire pancreas was divided into regional segments of pancreatic head, body, and tail. For pancreas with type 1 and type 2 image pattern, ROIs were made to cover the lesion only, if the measured segment was considered involved. Otherwise, the ROI was made to cover the whole segment, avoiding adjacent structures and dilated pancreatic duct (if present). For pancreas with type 3 and type 4 image pattern, ROIs were made to cover the whole pancreatic head, body, and tail, separately.

After a 2-week interval, the two radiologists evaluated the conventional MR sequences of the patients independently. The image sets were also randomized and blinded. For each

Table 1 Sequence parameters of the pancreatic MRI protocol

Sequence	Plane	Acquisition	TR/TE (ms)	FA (°)	Section thickness (mm)	FOV (mm)	Acquisition time (s)
T1w-VIBE-Dixon	Axial	BH	4.11/1.31–2.54	12	3	380×380	17
T2w-TSE FS	Axial	NT	2390/81	90	6	400×400	300–400
T2w- HASTE	Axial	NT	2000/92	90	4	300×300	120–180
T2w- HASTE	Coronal	NT	2000/92	90	4	300×300	120–180
ss-EPI-DWI	Axial	NT	2500/61	–	4	400×400	180–240
3D MRCP	Coronal	NT	1700/425	105	1	384×384	120–180
2D thick-slab MRCP	Para-coronal	BH	4500/735	180	60	400×400	3×3–6 orientations
3D-EPI-tomoelastography	Axial	FB	3270/69	–	2	256×256	240–300
TWIST-VIBE DCE	Axial	BH	3.89/1.23–2.46	10	3	400×400	600, multi-phase enhanced imaging

VIBE, volume-interpolated breath-hold; *TSE*, turbo spin-echo; *FS*, fat-saturated; *HASTE*, half-Fourier acquisition single-shot turbo spin-echo; *EPI*, echo planar imaging; *DWI*, diffusion-weighted imaging; *MRCP*, magnetic resonance cholangiopancreatography; *TWIST*, time-resolved imaging with interleaved stochastic trajectories; *DCE*, dynamic contrast enhanced

case, a 5-point diagnostic score (1, definitely PDAC; 2, probably PDAC; 3, indeterminate; 4, probably AIP; 5, definitely AIP) was given, based on known imaging findings that could help distinguishing the two disease entities [13–16].

Statistical analysis

Continuous data was tested for normal distribution with the Shapiro-Wilk test and expressed as means ± standard deviation if normally distributed. Categorical data was expressed as frequencies or percentages.

Interobserver agreement was assessed by the intraclass correlation coefficient (ICC) and Bland-Altman analysis. An ICC value of greater than 0.75 was considered a good agreement [27].

The stiffness and fluidity of PDAC, AIP, and healthy pancreas were compared using the Kruskal-Wallis test, with the post hoc Bonferroni correction for multiple testing.

Receiver operating characteristic (ROC) analysis was performed to determine and compare the diagnostic performance of tomoelastography and conventional MRI. The area under the curves (AUC) was calculated, and cutoff values were selected based on Youden's index. Area under the curve (AUC) was analyzed using the Hanley McNeil method [28].

The statistical analyses were performed using the MedCalc software (MedCalc Software Ltd) and GraphPad Prism (GraphPad Prism for Windows, version 5.01). A double-sided $p < 0.05$ indicated a statistically significant difference.

Results

The study included 40 patients with untreated pancreatic cancer (24 males, age range 26–78 years, median 58 years), 33 patients with untreated AIP (26 males, age range 37–77 years, median years 60 years), and 10 healthy volunteers (7 males, age range 28–65 years, median 52 years). There was no significant difference concerning gender ($p = 0.226$) and age ($p = 0.307$) among the groups.

In patients with PDAC, 19 tumors were located in the pancreatic head and 21 tumors in the pancreatic body-tail. Nineteen patients received curative-intent surgery, and 21 patients received biopsy followed by adjuvant therapy due to locally advanced cancer or metastases found at diagnosis.

In patients with AIP, 21 had diffuse pancreatic involvement, 2 had multi-focal involvement, and 10 had single-focal involvement. All the patients received steroid therapy with clinical and radiological improvement.

Interobserver variability of tomoelastography

The technical setup, data acquisition, and postprocessing were successful in all participants.

ICCs of pancreatic stiffness were 0.976 (95% confidence interval [CI]: 0.968 to 0.982) between reader 1 and reader 2, 0.958 (95% CI: 0.944 to 0.968) between reader 1 and reader 3, and 0.979 (95% CI: 0.972 to 0.984) between reader 2 and reader 3, indicating near-perfect interobserver agreement (all $p < 0.001$).

ICCs of pancreatic fluidity were 0.951 (95% CI: 0.939 to 0.967) between reader 1 and reader 2, 0.974 (95% CI: 0.963 to 0.982) between reader 1 and reader 3, and 0.963 (95% CI: 0.951 to 0.972) between reader 2 and reader 3, which also indicated near-perfect interobserver agreement (all $p < 0.001$).

Figure 1 shows the Bland-Altman analysis of pancreatic stiffness and fluidity measurement by reader 1 (senior radiologist) and reader 3 (technician).

Stiffness and fluidity characteristics of PDAC, AIP, and normal pancreas

In healthy subjects, pancreatic stiffness and fluidity did not differ among pancreatic head, body, and tail ($p = 0.64$ and $p = 0.71$, respectively).
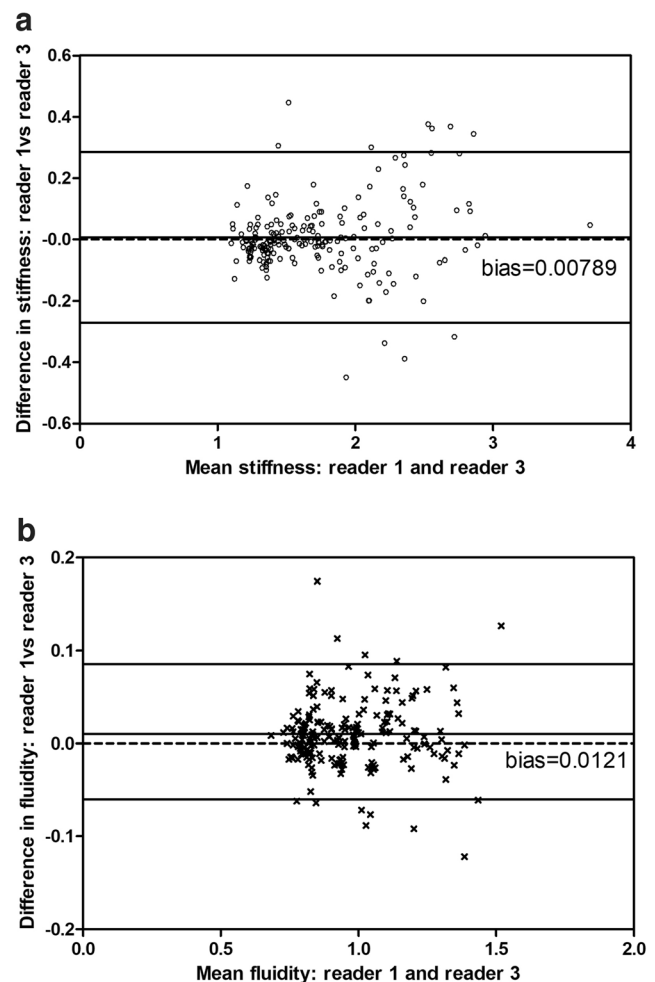

Fig. 1 Bland-Altman analysis of reader agreement (senior radiologist vs. technician) in pancreatic stiffness (**a**) and pancreatic fluidity measurement (**b**)

For patients with PDAC, 32 (80%) showed type 1 image pattern (signal-focal hotspot lesion) on stiffness map, and 8 (20%) showed type 3 image pattern (heterogeneous diffuse lesion). All the latter had tumors located in the pancreatic head.

For patients with AIP, all four involvement patterns were identified: 10 (30.3%) were type 1 (single-focal), 2 (6.1%) type 2 (multi-focal), 15 (45.5%) type 3 (heterogeneous diffuse), and 3 (9.1%) type 4 (homogeneous diffuse) lesions.

The group mean values and standard deviations of pancreatic stiffness and fluidity in PDAC, AIP, and healthy pancreas are shown in Table 2. The stiffness of PDAC (2.34 ± 0.39 m/s) was significantly higher compared to that of AIP (1.77 ± 0.15 m/s) and healthy pancreas (1.32 ± 0.05 m/s, both $p < 0.001$), while the stiffness of AIP was also higher compared to that of normal pancreas ($p < 0.001$).

Similarly, the fluidity of PDAC (1.20 ± 0.15 rad) was significantly higher compared to that of AIP (1.02 ± 0.13 rad) and healthy pancreas (0.81 ± 0.03, both $p < 0.001$), while the fluidity of AIP was also higher compared to that of normal pancreas ($p < 0.001$).

Figures 2 and 3 and supplement figures s1-s2 show examples of tomoelastography findings in patients with PDAC and AIP.

Scatterplots of group values of pancreatic stiffness and fluidity of PDAC, its proximal and distal parenchyma, and AIP are shown in Fig. 4. While the parenchyma proximal to PDAC (i.e., parenchyma on the right side of the tumor, towards the direction of the pancreatic head) had a stiffness of 1.29 ± 0.09 m/s, similar to normal pancreas (1.32 ± 0.05 m/s, $p = 0.374$), the parenchyma distal to PDAC (i.e., parenchyma on the left side of the tumor, towards the direction of the pancreatic tail) was significantly stiffer than the normal pancreas (1.65 ± 0.34 m/s, $p < 0.001$). On the contrary, the pancreatic parenchyma proximal and distal to PDAC did not show significant difference in fluidity (0.83 ± 0.05 and 0.86 ± 0.07, $p = 0.167$).

Diagnostic accuracy of tomoelastography and conventional MR sequences

The diagnostic performance of the 3 readers using pancreatic stiffness, fluidity, and conventional MRI are shown in Table 3. The AUCs with pancreatic stiffness and fluidity were not significantly different among the three readers (all $p > 0.20$), regardless of the background of diagnostic training and experience.

For the senior radiologist, diagnostic accuracy with pancreatic stiffness was high, with an AUC of 0.906, and diagnostic accuracy with pancreatic fluidity was also satisfactory, with an AUC of 0.872. Diagnostic accuracy with conventional MRI findings was slightly lower with an AUC of 0.842, but the difference was not significant ($p = 0.392$ and 0.660 compared to pancreatic stiffness and fluidity, respectively). For the junior radiologist, a similar trend was found, with AUCs of 0.912, 0.869, and 0.828 for pancreatic stiffness, fluidity, and diagnosis derived from conventional MRI, respectively. The differences were not significant.

Discussion

To the best of our knowledge, this is the first report on the tomographic mapping of stiffness and fluidity for characterizing pancreatic lesions. We found that elevated pancreatic stiffness and fluidity allowed separation of PDAC from AIP and normal pancreas with high diagnostic accuracy. Tomoelastography provides high-resolution parameter maps,

Table 2 Pancreatic stiffness and fluidity in PDAC, AIP, and normal pancreas, as measured by the 3 readers

|	Reader 1 (senior radiologist)	Reader 2 (resident radiologist)	Reader 3 (technician)	p value reader 1 vs 2	p value reader 1 vs 3	p value reader 2 vs 3
Stiffness measurement (m/s)						
Pancreatic cancer	2.35 ± 0.39	2.33 ± 0.42	2.31 ± 0.41	0.275	0.083	0.621
Downstream (uninvolved) pancreas	1.29 ± 0.09	1.31 ± 0.13	1.30 ± 0.10	0.085	0.179	0.724
Upstream pancreas	1.65 ± 0.34	1.65 ± 0.40	1.63 ± 0.38	0.772	0.215	0.093
Autoimmune pancreatitis	1.77 ± 0.15	1.76 ± 0.16	1.77 ± 0.16	0.324	0.596	0.832
Healthy pancreas	1.32 ± 0.05	1.32 ± 0.06	1.32 ± 0.05	0.377	0.507	0.827
Fluidity measurement (rad)						
Pancreatic cancer	1.20 ± 0.13	1.20 ± 0.16	1.19 ± 0.16	0.535	0.326	0.609
Downstream (uninvolved) pancreas	0.83 ± 0.05	0.82 ± 0.05	0.82 ± 0.04	0.822	0.418	0.791
Upstream pancreas	0.86 ± 0.07	0.85 ± 0.08	0.86 ± 0.09	0.274	0.621	0.188
Autoimmune pancreatitis	1.02 ± 0.13	1.02 ± 0.14	1.02 ± 0.13	0.231	0.539	0.554
Healthy pancreas	0.81 ± 0.04	0.80 ± 0.04	0.80 ± 0.03	0.126	0.473	0.443
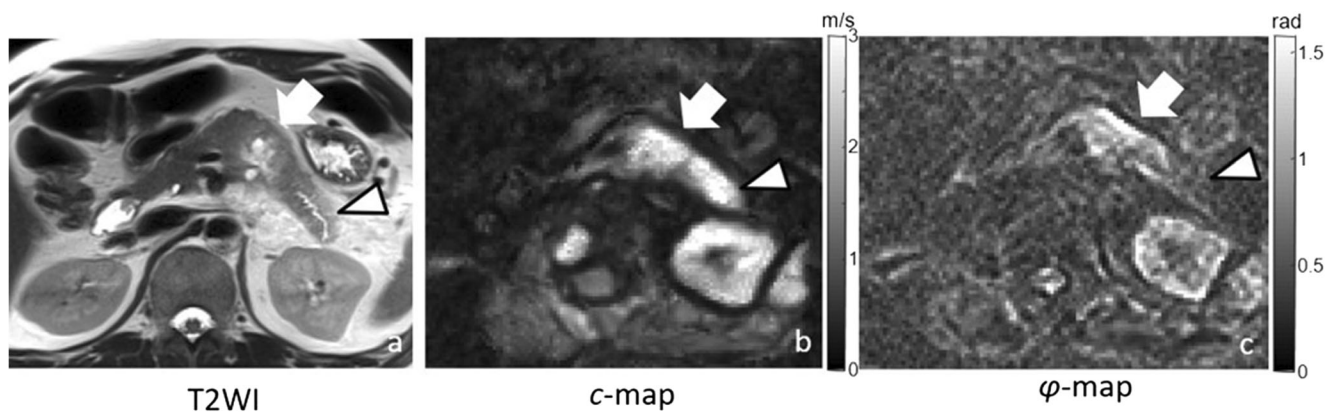
Fig. 2 A 43-year-old male patient with biopsy-proven pancreatic ductal adenocarcinoma. **a** Axial T2-weighted image shows a heterogeneous high-signal-intensity mass lesion in the pancreatic body (arrow), with upstream pancreatic duct dilation and distal parenchyma atrophy (arrowhead). **b** On the tomoelastographic *c* map, which characterizes pancreatic stiffness, the tumor in the pancreatic body (arrow) and the distal pancreatic parenchyma (arrowhead) both showed increased stiffness, and the tumor border was unclear. **c** On the tomoelastographic φ map, which characterizes pancreatic fluidity, only the tumor in the pancreatic body (arrow) showed increased fluidity, while the distal pancreatic parenchyma (arrowhead) did not

which facilitates ROI selection [25, 29–31], enabling even less-experienced users to quantify the mechanical characters of the pancreas. It has been shown that diagnostic accuracy of AIP based on radiological signs could be quite low with inexperienced readers, as investigated by Sugumar et al, with the famous comment "the eyes do not see what the mind does not know" [17]. The inter-reader agreement from subjective interpretation of images may be another problem. A multi-reader study of CT signs for characterizing AIP had kappa values varying from 0.28 to 0.75, some of which were far from satisfactory [32]. In our study, interobserver agreement for pancreatic stiffness and fluidity measurement was near-perfect among the three readers, and the diagnostic accuracy achieved by the technician was similar to the senior radiologist. These results suggest that the determination of mechanical properties is reader-independent. Moreover, the measurement of mechanical properties does not require extensive training. The

quantitative information provided by tomoelastography could be very useful for institutions other than specialized tertiary centers. In our study, the diagnostic accuracy with tomoelastography was higher than 0.90 by all readers, which was superior compared to the subjective interpretation by the senior radiologist. This diagnostic accuracy increment means that more patients who are suspected of having pancreatic cancer or AIP will be saved from an indeterminate or wrong diagnosis at the first place. Since the diagnosis of a totally benign disease or a highly lethal malignancy means "heaven or hell" for the patient and family, a correct diagnosis from non-invasive examination will save a long torturous experience of waiting and multiple invasive procedures.

It is interesting to note that, in patients with PDAC, increased tissue stiffness was observed not only in the tumor itself but also in the pancreatic parenchyma distal to the tumor. In our study, 8 cases (20%) of pancreatic cancer were interpreted as diffuse,
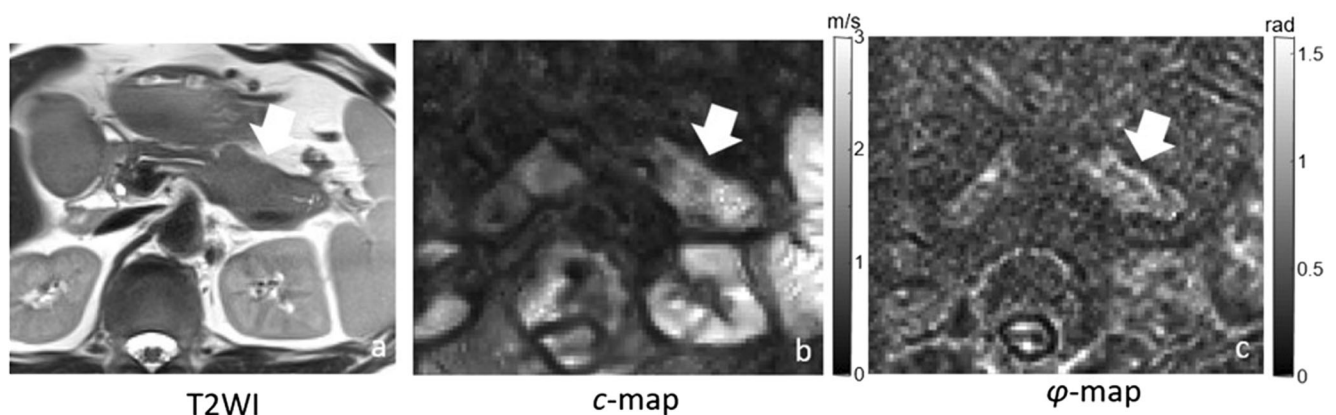

Fig. 3 A 57-year-old male patient with IgG4-related autoimmune pancreatitis, which involved the pancreatic body and tail. **a** Axial T2-weighted image shows mass-like swelling of the pancreatic body and tail (arrow), with slightly increased signal intensity. **b** On the tomoelastographic *c* map, AIP showed increased stiffness (arrow), which was lower compared to typical pancreatic cancer. **c** On the tomoelastographic φ map, which characterizes pancreatic fluidity, AIP showed increased fluidity (arrow), which was also lower compared to typical pancreatic cancer
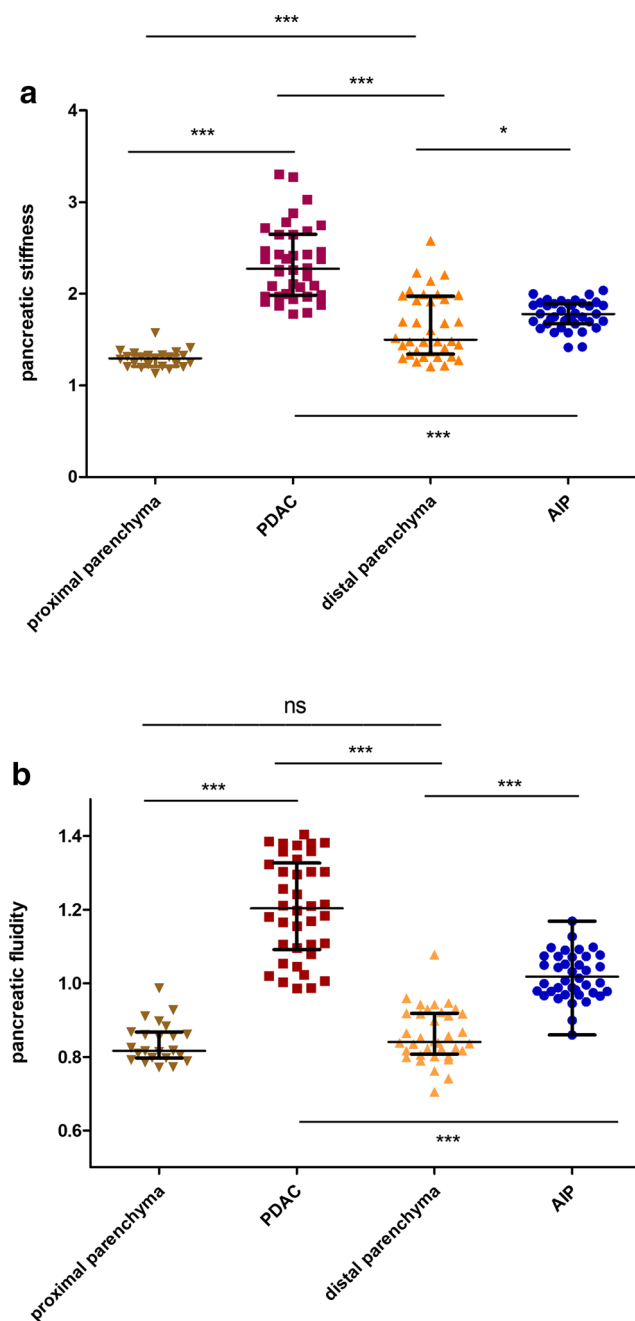
Fig. 4 Scatterplots showing the pancreatic stiffness (**a**) and fluidity (**b**) in pancreatic cancer, its proximal and distal parenchyma (pancreatic parenchyma on the right and left side of the tumor, respectively), and in AIP. PDAC had higher stiffness and fluidity compared to AIP. The pancreatic parenchyma distal to PDAC showed increased stiffness, while the parenchyma proximal to PDAC was normal. The pancreatic parenchyma distal and proximal PDAC showed no significant difference in fluidity. (*** denotes $p < 0.001$, * denotes $0.01 < p < 0.05$, and ns denotes no significant difference)

heterogenous pancreatic involvement on the stiffness map. All such lesions were located in the pancreatic head. Invasion of ductal epithelium by the tumor causes mechanical obstruction and upstream dilation of the pancreatic ducts, which appear as secondary signs of pancreatic cancer. At histopathological

analysis, the presence of acute pancreatitis in the pancreatic parenchyma distal to pancreatic cancer was high (70%) [33]. This is probably caused by the increased pressure within the ducts and stasis of pancreatic juice [34], which exerts a force onto the distal parenchyma tissue, leading to increased stiffness. On the contrary, the fluidity of the pancreatic parenchyma distal to PDAC is not influenced, suggesting that the microenvironment of the pancreatic parenchyma remained stable and there was little change of solid-fluid biomechanical property of the parenchyma by obstructive changes. Since fluidity increase is only responsive to malignancy, not to secondary obstructive changes, it adds specificity to the characterization of pancreatic cancer.

Pancreatic stiffness is quite sensitive to the inflammatory change. It has been reported that MRE could detect acute pancreatitis at a very early stage, with a higher sensitivity compared to contrast-enhanced CT [35]. Although the median pancreatic stiffness value for acute pancreatitis was lower, its range has considerable overlap with other pancreatic diseases including pancreatic cancer [20, 36, 37]. Shi et al have attempted to combine the stiffness value and the pancreatic involvement pattern on elastogram to increase the diagnostic accuracy for differentiating AIP from PDAC. In their report, most patients with pancreatic cancer manifested as solitary high-stiffness lesions. In our study, however, the presence of a pseudo-diffuse lesion on the stiffness map was more common (20%) and could not be ignored. This might be explained by the selection bias, since Shi's study only included resectable pancreatic cancer.

The fact that pancreatic stiffness is sensitive to both inflammatory change and malignancy might cause problems in the clinical settings. Pancreatic cancer with secondary acute pancreatitis could have been overlooked or misdiagnosed, in the background of diffuse inflammatory change. In contrast, pancreatic fluidity is a more specific marker for malignancy, and combining both stiffness and fluidity could help ruling out tumor-caused obstruction when diagnosing patients suffering from acute pancreatitis without known risk factors.

Fluidity reflects the internal mechanical friction of biological tissue, rather than its gross water content [21]. Research on liver tumors found that fluidity may serve as a biomarker for aggressiveness and invasiveness [22]. Several events during pancreatic cancer development and progression might contribute to the increased fluidity, such as activation of stellate cells and accumulation of hydrophobic proteins within the tumor extracellular matrix, the depletion of glycosaminoglycans, and change in collagen content which turned from an organized chained pattern to a more randomly aligned pattern [21, 22].

Our study has several limitations. First, it is a single-institutional study carried out in a tertiary pancreatic disease center. Institutional bias might exist, and a multi-center validation study is required to confirm our results. Second, since AIP is a benign inflammatory disease, a

Table 3 Diagnostic performances of pancreatic stiffness, fluidity, and subjective interpretation of MR images in differentiating pancreatic ductal adenocarcinoma and autoimmune pancreatitis

	Reader 1 (senior radiologist)		Reader 2 (resident radiologist)		Reader 3 (technician)	
	Cutoff	AUC value	Cutoff	AUC value	Cutoff	AUC value
Pancreatic stiffness (m/s)	1.917	0.906	1.911	0.912	1.913	0.906
Pancreatic fluidity (rad)	1.098	0.872	1.107	0.869	1.098	0.881
Subjective score from MR images interpretation	2	0.842	2	0.828	–	–

direct correlation with pathological features was not possible. To better understand the relationship between mechanical properties and AIP histopathology, a longitudinal study involving observation of treatment response is warranted. Third, it was deduced that obstructive change was the reason for increased stiffness in the distal parenchyma of pancreatic cancer, but pathological confirmation of acute pancreatitis was not performed.

In conclusion, tomoelastography facilitated an easy, unbiased, and user-independent analysis of the mechanical properties of the pancreas, allowing differentiation of PDAC from AIP with high accuracy.

Compliance with ethical standards

Guarantor The scientific guarantor of this publication is Professor Ingolf Sack from the Department of Radiology, Charité-universitätsmedizin Berlin.

Conflict of interest The authors of this manuscript declare no relationships with any companies whose products or services may be related to the subject matter of the article.

Statistics and biometry No complex statistical methods were necessary for this paper.

Informed consent Written informed consent was obtained from all subjects (patients) in this study.

Ethical approval Institutional Review Board approval was obtained.

Methodology
• Prospective
• Diagnostic study
• Performed at one institution

References

1. Moffat GT, Epstein AS, O'Reilly EM (2019) Pancreatic cancer-a disease in need: optimizing and integrating supportive care. Cancer. 125(22):3927–3935

2. Dickerson LD, Farooq A, Bano F et al (2019) Differentiation of autoimmune pancreatitis from pancreatic Cancer remains challenging. World J Surg 43(6):1604–1611

3. Saavedra-Perez D, Vaquero EC, Ayuso JR et al (2014) Autoimmune pancreatitis: a surgical dilemma. Cir Esp 92(10): 645–653

4. Khandelwal A, Inoue D, Takahashi N (2020) Autoimmune pancreatitis: an update. Abdom Radiol 45(5):1359–1370

5. Luo G, Liu C, Guo M et al (2017) Potential biomarkers in Lewis negative patients with pancreatic cancer. Ann Surg 265(4):800–805

6. Ballehaninna UK, Chamberlain RS (2012) The clinical utility of serum CA 19-9 in the diagnosis, prognosis and management of pancreatic adenocarcinoma: an evidence based appraisal. J Gastrointest Oncol 3(2):105–119

7. Martins C, Lago P, Sousa P et al (2017) Type 2 autoimmune pancreatitis: a challenge in the differential diagnosis of a pancreatic mass. GE Port J Gastroenterol 24(6):296–300

8. Ngwa T, Law R, Hart P et al (2015) Serum IgG4 elevation in pancreatic cancer: diagnostic and prognostic significance and association with autoimmune pancreatitis. Pancreas 44(4):557–560

9. Ghazale A, Chari ST, Smyrk TC et al (2007) Value of serum IgG4 in the diagnosis of autoimmune pancreatitis and in distinguishing it from pancreatic cancer. Am J Gastroenterol 102(8):1646–1653

10. Zaheer A, Singh VK, Akshintala VS et al (2014) Differentiating autoimmune pancreatitis from pancreatic adenocarcinoma using dual-phase computed tomography. J Comput Assist Tomogr 38(1):146–152

11. Furuhashi N, Suzuki K, Sakurai Y et al (2015) Differentiation of focal-type autoimmune pancreatitis from pancreatic carcinoma: assessment by multiphase contrast-enhanced CT. Eur Radiol 25(5): 1366–1374

12. Muhi A, Ichikawa T, Motosugi U et al (2012) Mass-forming autoimmune pancreatitis and pancreatic carcinoma: differential diagnosis on the basis of computed tomography and magnetic resonance cholangiopancreatography, and diffusion-weighted imaging findings. J Magn Reson Imaging 35(4):827–836

13. Sun GF, Zuo CJ, Shao CW et al (2013) Focal autoimmune pancreatitis: radiological characteristics help to distinguish from pancreatic cancer. World J Gastroenterol 19(23):3634–3641

14. Kim HJ, Kim YK, Jeong WK et al (2015) Pancreatic duct "icicle sign" on MRI for distinguishing autoimmune pancreatitis from pancreatic ductal adenocarcinoma in the proximal pancreas. Eur Radiol 25(6):1551–1560

15. Choi SY, Kim SH, Kang TW et al (2016) Differentiating mass-forming autoimmune pancreatitis from pancreatic ductal adenocarcinoma on the basis of contrast-enhanced MRI and DWI findings. AJR Am J Roentgenol 206(2):291–300

16. Hur BY, Lee JM, Lee JE et al (2012) Magnetic resonance imaging findings of the mass-forming type of autoimmune pancreatitis: comparison with pancreatic adenocarcinoma. J Magn Reson Imaging 36(1):188–197

17. Sugumar A, Levy MJ, Kamisawa T et al (2011) Endoscopic retrograde pancreatography criteria to diagnose autoimmune pancreatitis: an international multicentre study. Gut 60(5):666–670

18. Apte MV, Park S, Phillips PA et al (2004) Desmoplastic reaction in pancreatic cancer: role of pancreatic stellate cells. Pancreas 29(3): 179–187

19. Zamboni G, Luttges J, Capelli P et al (2004) Histopathological features of diagnostic and clinical relevance in autoimmune pancreatitis: a study on 53 resection specimens and 9 biopsy specimens. Virchows Arch 445(6):552–563

20. Shi Y, Cang L, Zhang X et al (2018) The use of magnetic resonance elastography in differentiating autoimmune pancreatitis from pancreatic ductal adenocarcinoma: a preliminary study. Eur J Radiol 108:13–20

21. Streitberger KJ, Lilaj L, Schrank F et al (2020) How tissue fluidity influences brain tumor progression. Proc Natl Acad Sci U S A 117(1):128–134

22. Shahryari M, Tzschatzsch H, Guo J et al (2019) Tomoelastography distinguishes noninvasively between benign and malignant liver lesions. Cancer Res 79(22):5704–5710

23. Tzschatzsch H, Guo J, Dittmann F et al (2016) Tomoelastography by multifrequency wave number recovery from time-harmonic propagating shear waves. Med Image Anal 30:1–10

24. Streitberger KJ, Diederichs G, Guo J et al (2015) In vivo multifrequency magnetic resonance elastography of the human intervertebral disk. Magn Reson Med 74(5):1380–1387

25. Marticorena Garcia SR, Grossmann M, Bruns A et al (2019) Tomoelastography paired with T2* magnetic resonance imaging detects lupus nephritis with normal renal function. Invest Radiol 54(2):89–97

26. Bertalan G, Guo J, Tzschatzsch H et al (2019) Fast tomoelastography of the mouse brain by multifrequency single-shot MR elastography. Magn Reson Med 81(4):2676–2687

27. Hallgren KA (2012) Computing inter-rater reliability for observational data: an overview and tutorial. Tutor Quant Methods Psychol 8(1):23–34

28. Hanley JA, McNeil BJ (1982) The meaning and use of the area under a receiver operating characteristic (ROC) curve. Radiology 143(1):29–36

29. Hudert CA, Tzschatzsch H, Rudolph B et al (2019) Tomoelastography for the evaluation of pediatric nonalcoholic fatty liver disease. Invest Radiol 54(4):198–203

30. Lang ST, Guo J, Bruns A et al (2019) Multiparametric quantitative MRI for the detection of IgA nephropathy using Tomoelastography, DWI, and BOLD imaging. Invest Radiol 54(10):669–674

31. Marticorena Garcia SR, Fischer T, Durr M et al (2016) Multifrequency magnetic resonance elastography for the assessment of renal allograft function. Invest Radiol 51(9):591–595

32. Takahashi N, Fletcher JG, Fidler JL et al (2008) Dual-phase CT of autoimmune pancreatitis: a multireader study. AJR Am J Roentgenol 190(2):280–286

33. Fukukura Y, Takumi K, Kamimura K et al (2012) Pancreatic adenocarcinoma: variability of diffusion-weighted MR imaging findings. Radiology 263(3):732–740

34. Mujica VR, Barkin JS, Go VL (2000) Acute pancreatitis secondary to pancreatic carcinoma. Study Group Participants. Pancreas 21(4): 329–332

35. Shi Y, Liu Y, Liu YQ et al (2017) Early diagnosis and severity assessment of acute pancreatitis (AP) using MR elastography (MRE) with spin-echo echo-planar imaging. J Magn Reson Imaging 46(5):1311–1319

36. Liu Y, Wang M, Ji R et al (2018) Differentiation of pancreatic ductal adenocarcinoma from inflammatory mass: added value of magnetic resonance elastography. Clin Radiol 73(10):865–872

37. Shi Y, Gao F, Li Y et al (2018) Differentiation of benign and malignant solid pancreatic masses using magnetic resonance elastography with spin-echo echo planar imaging and three-dimensional inversion reconstruction: a prospective study. Eur Radiol 28(3):936–945